agriculture

Article

Estimation of Total Nitrogen Content in Forage Maize (*Zea mays* L.) Using Spectral Indices: Analysis by Random Forest

Magali J. López-Calderón [1], Juan Estrada-Ávalos [2,*], Víctor M. Rodríguez-Moreno [3], Jorge E. Mauricio-Ruvalcaba [3], Aldo R. Martínez-Sifuentes [2], Gerardo Delgado-Ramírez [2] and Enrique Miguel-Valle [2]

1 Facultad de Agricultura y Zootecnia (FAZ-UJED), Universidad Juárez del Estado de Durango, Ejido Venecia, Tlahualilo Km 35, Gómez Palacio 35111, Mexico; magali.lopezcalderon@gmail.com

2 INIFAP CENID-RASPA, Km 6.5 márgen derecho del canal del Sacramento, Gómez Palacio 35140, Mexico; im_aldo09@hotmail.com (A.R.M.-S.); delgado.gerardo@inifap.gob.mx (G.D.-R.); quiquemiguel89@hotmail.com (E.M.-V.)

3 INIFAP Campo Experimental Pabellón, Km 32.5, Carretera Ags-Zac, Pabellón de Arteaga 20660, Mexico; rmoreno.victor@gmail.com (V.M.R.-M.); jorge.ernesto.mauricio@gmail.com (J.E.M.-R.)

* Correspondence: estrada.juan@inifap.gob.mx; Tel.: +52-87-1346-1656

Received: 5 August 2020; Accepted: 18 September 2020; Published: 1 October 2020

Abstract: Knowing the total Nitrogen content (Nt) of forage maize (*Zea mays*) is important so that decisions can be made quickly and efficiently to adjust the timing and amount of both irrigation and fertilizer. In 2017 and 2018 during three growing cycles in two study plots, leaf samples were collected and the Dumas method was used to estimate Nt. During the same growing seasons and on the same sampling plots, a Parrot Sequoia camera mounted on an unmanned aerial vehicle (UAV) was used to collect high resolution images of forage maize study plots. Thirteen multispectral indices were generated and, from these, a Random Forest (RF) algorithm was used to estimate Nt. RF is a machine-learning technique and is designed to work with extremely large datasets. Overall analysis showed five of the 13 indices as the most important. One of these five, the Transformed Chlorophyll Absorption in Reflectance Index/Optimized Soil-Adjusted Vegetation Index, was found to be the most important for estimation of Nt in forage maize (R^2 = 0.76). RF handled the complex dataset in a time-efficient manner and Nt did not differ significantly when compared between traditional methods of evaluating Nt at the canopy level and using UAVs and RF to estimate Nt in forage maize. This result is an opportunity to explore many new research options in precision farming and digital agriculture.

Keywords: nitrogen content; remote sensing; spectral indices; random forest

1. Introduction

Nitrogen (N), in both its organic and inorganic forms, is essential to promote leaf development and crop growth. Nitrogen is present in the soil in two ways: the decomposition of plants naturally high in N such as legumes, buckwheat, and others (organic N; amino acids, proteins, and nucleotides), and the human application of fertilizer (inorganic N; (ammonium [NH_4^+], nitrates [NO_3^-], Nitrogen gas [N_2], and nitrites [NO_2^-])).

Maize (*Zea mays*) has one of the highest photosynthetic rates per unit of N [1] and is thus considered a C4 plant. The N content in maize determines the yield and quality of grain and must be available in the soil in adequate quantities throughout the growing season. Vos et al. [2] noticed a 29% increase in the foliar area when compared to a high versus low incorporated amount of N in the soil. A lack of N results in an inefficient photosynthesis process because it is a fundamental constituent element in the chlorophyll molecule [3].

Chlorophyll absorbs the necessary sunlight energy to catalyze the photosynthetic process and is the pigment responsible for the green color of leaves. Its content in leaves relates to the amount of N in a crop [4]. A less than optimal N content manifests itself in light green or yellowing leaves (chlorosis) [5].

One way to determine the total N content (Nt) in plants is to use the reflectance data on red edge (RE) wavelengths [6]. A consensus on N content is that the physical expression of chlorosis is related by an increase in the reflectance value of the visible spectrum and a decrease in the absorption of the near-infrared (NIR) region [7].

The indirect estimation of Nt is attainable through spectral indices [3,8]. Some authors have reported the close relationship among the indices with chlorophyll content [9]. In conjunction with a sampling field design, and a follow-up growing season practices program, they are a reliable alternative to estimate Nt to reduce cost and time in decision-making [10–12].

Remote sensing images have become attractive in digital agriculture and precision farming as they are used to monitor crop growth rapidly and in a nondestructive way [13]. The optical sensors carried by manned and unmanned air vehicles were designed to register a wide range of high spatial resolution for data collection of crops' dynamic nature. The satellite images are an excellent option [5,6] to monitor the N status on large plant cover areas. Despite their low spatial resolution and large temporal resolution, thematic maps provide sufficient accuracy. Even though manned and unmanned air vehicles can capture images at higher spatial and temporal resolutions than the satellite-origin, but they are limited by their high operational complexity and cost [7]. Digital agriculture stands its operational bases on the use of free access multispectral satellite-origin images, as Landsat, Sentinel, SPOT, and MODIS. The unmanned aerial vehicle (UAV; also known as a drone) is expanding its use to refine the multispectral bands to register only the ones most associated with the plant physiologic processes. These images have technical advantages over satellite platforms, such as (a) a better spatial resolution (the pixel size may vary based on the flight height, and can reach up to 1 cm); (b) high temporal resolution—several flights can be programmed at any time during the day.

Operational limitations in using drones include the difficulty of flying in extreme weather conditions of wind, rain, and high air temperatures, low-scale coverage due to high data volume and limited image storage capacity, and the data download and processing time. The most technically advanced drones currently have several options for mission planning schedules, pre- and postprocessing of images, autonomous flight, and coupling cameras with optical sensors or radar [14].

An important achievement in remote sensing data science the estimation of the chlorophyll content in leaves by contrasting the NIR and RE wavelengths; these wavelengths represent the wide variation of reflected energy by the canopy, and the point of maximum slope in vegetation reflectance spectra, which occurs between wavelengths 690 and 740 nm [15–17]. This band ratio results in a numerical value that indicates how sunlight energy interacts with vegetation cover (the amount that was reflected, absorbed, or was transferred to the soil). The RE point wavelength is well correlated with the chlorophyll content in the leaves [18]. It marks the threshold between the processes of chlorophyll absorption in red wavelengths and within-leaf scattering in the NIR [19]. The RE emphasizes the lower absorption of chlorophyll, which reduces the saturation effect; however, the reflectance value continues to be sensitive to chlorophyll absorption in moderate to high values [8,20].

Some studies have documented the relationship between the RE and the chlorophyll content in maize [3,6,8,21,22] and have proposed a number of indices that enhanced this ratio—the GNDVI (Green Normalized Difference Vegetation Index), CI_green (Chlorophyll Index Green), NDVI (Normalized Difference Vegetation Index), RVI (Ratio Vegetation Index), NDRE (Normalized Difference Red Edge), CCCI (Canopy Chlorophyll Content Index), CI_rededge (Red edge Chlorophyll Index), MCARI/OSAVI (Modified Chlorophyll Absorption in Reflectance Index/Optimized Soil-Adjusted Vegetation Index), MCARI/OSAVI RE (Red Edge-based Modified Chlorophyll Absorption in Reflectance Index/Optimized

Soil Adjusted Vegetation Index), TCARI/OSAVI (Transformed Chlorophyll Absorption in Reflectance Index/Optimized Soil-Adjusted Vegetation Index), TCARI/OSAVI RE (Red Edge-based Transformed Chlorophyll Absorption in Reflectance Index/Optimized Soil Adjusted Vegetation Index), and MTCI (MERIS Terrestrial Chlorophyll Index) among others. One common result reported by researchers is that these indices tend to exhibit saturation values in moderate to high plant cover [6,23,24], but discussing this situation is out of the reach of this manuscript.

We used these indices to show internal and external relationships between vegetation cover and its response to sunlight. The use of data mining, deep learning, and other data analysis techniques can help to recognize patterns and trends that cannot be seen without these analyses. Among these techniques are decision trees (DTs), Random Forest (RF), support vector machine, and artificial neural networks, all of which perform quite well with very large databases and in current approaches involving plant nutritional status [25], water-demand [26], biomass [27], and chlorophyll content [28]. When the results of any data analysis failed to find a strong relationship between or among variables, the RF analysis may be a viable option [29]. RF is a nonparametric analysis that uses DTs, with their class values assigned according to the maximum number of forecast votes through the DTs [30], and with more predictive power in comparison to classic regression methods [31,32], in essence to efficiently handling many variables that do not adjust to a normal distribution.

We compared the collection and analysis of Nt in forage maize with the industry-standard method versus the collection of multispectral images and RF analysis. To our knowledge, there are no published studies that used UAV-collected multispectral data to estimate total Nt in combination with the RF algorithm for data analysis; therefore, the use of UAV imagery and RF in this context is innovative and will contribute to future research.

2. Materials and Methods

2.1. Description of the Study Areas

The study areas are in the north-central region of Mexico known as the Comarca Lagunera (Figure 1). The cultivated area of forage maize has been reported at approximately 59,298 ha [33]. This semidesert to arid region has a mean annual temperature of 20–22 °C and mean annual precipitation of 200–300 mm.

2.2. Description of Sampling Sites

Two large agricultural farms were studied (Granada and El Porvenir; Figure 1). The Granada farm was studied during the summer–autumn forage maize production cycle in 2017, while in 2018, the spring–summer and summer–autumn cycles were evaluated at El Porvenir.

The Granada farm occupies an area of 60.4 ha. The soil composition is clay-loam. The maize hybrid sown was Pioneer P3201 and was selected because it is a hybrid of early to intermediate varieties, it has high nutritional content when used as forage for dairy cattle, high grain health, and high tolerance to root and/or stem lodging. Eight seeds meter^{-1} will produce a density of 103,000 plants ha^{-1}. The agricultural management practices included fallowing, harrow passing, skirting, and leveling (slope of 2 cm per 100 m). Chemical fertilizer was applied two times. The first application was composed of 42% ammonium sulfate, 42% monoammonium phosphate, and 16% Ryzogen (a granular microbial fertilizer used to stimulate root growth); this was incorporated into the soil at the time of sowing at a rate of 250 kg ha^{-1}. The second time was immediately after the first additional water had been applied; the fertilizer consisted of urea (46%) at 400 kg ha^{-1}. The irrigation schedule included five additional dates. The maize was harvested 117 days after sowing (DAS) when the forage reached 32% of dry matter content.

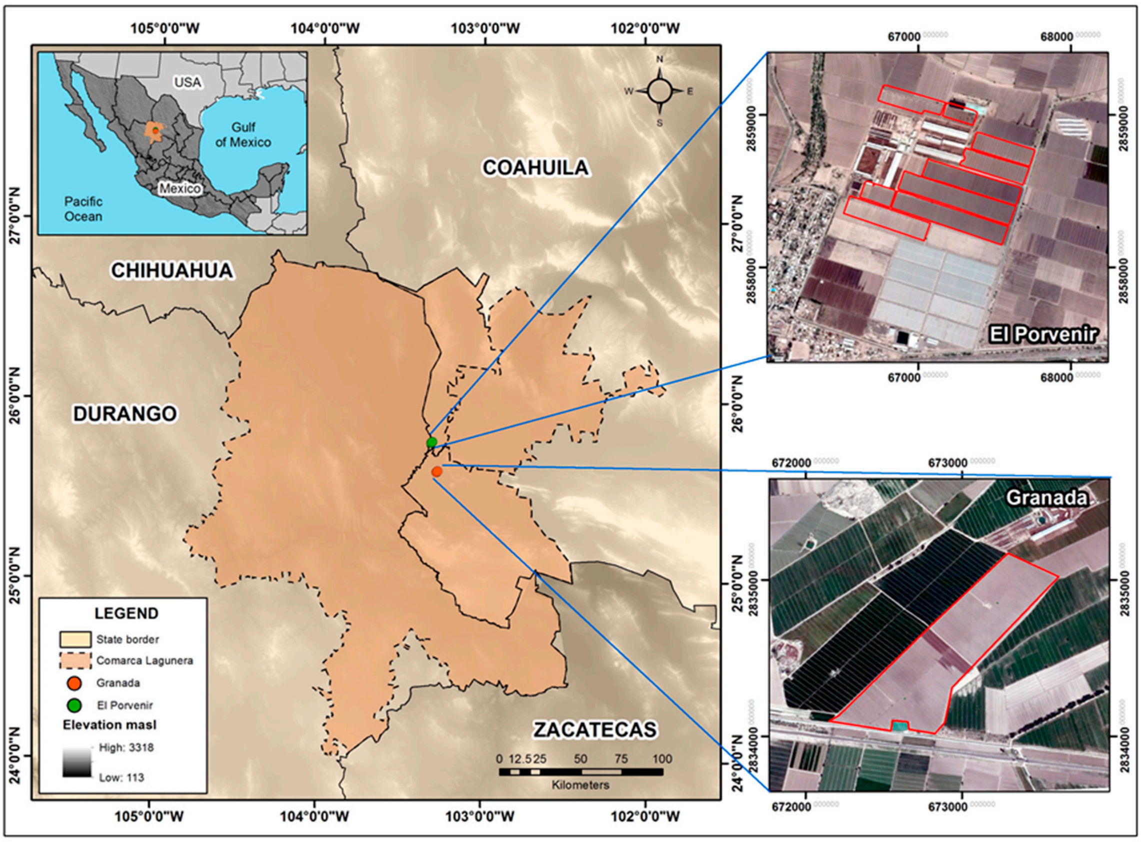

Figure 1. Study area location. The sample sites were recorded with a geographical information system.

On the El Porvenir site, 52 ha of forage maize was studied in the spring–summer cycle, and 34 ha in the summer–autumn cycle; this variation has no effect on the number of plant samples. The Syngenta N83N5 maize hybrid was sown in loam-clay soil at the same density as at the Granada farm. This forage maize is an earlier cycle variety with high nutritional value and high stability in various soil types and performs well in different environments. This farm was handled with the same agricultural practices as the Granada farm (fallowing, harrow passing, skirting, and leveling). A sole application of a mixture of chemical fertilizer mixture was performed. It was composed of 300 kg ha^{-1} of ammonium sulfate and 100 kg ha^{-1} of monoammonium phosphate. The irrigation schedule included a total of four dates. Maize was harvested when it reached 38% of dry matter—at 118 DAS in spring–summer, and 115 DAS in summer–autumn.

2.3. Field Sampling

For both farms, we collected composite plant samples (CPSs) before and after flowering, and each collection site was georeferenced using a Garmin Etrex 20 geographic positioning system receiver, with a 3.6 m margin of error. Before flowering, samples were taken from three plants (stem and leaves) in the same plot, and after flowering samples were taken from the leaf opposite the ear of corn from ten plants. Plant samples were sent to the laboratory for further analysis.

For the Granada farm, there were six dates for plant collection samples each associated with aerial imaging planning. The first sampling was performed at 33 DAS with 15 CPSs; the second at 57 DAS with 19 CPSs; the third at 62 DAS with 18 CPSs; the fourth at 72 DAS with 16 CPSs; the fifth at 82 DAS with 18 CPSs; the sixth at 105 DAS with 17 CPSs.

For the El Porvenir farm, we scheduled three plant collection dates for each of the two cycles, and each was associated with an aerial imaging date. For the spring–summer cycle, the first sampling was performed at 31 DAS with 10 CPSs; the second at 41 DAS with 10 CPSs; the third at 51 DAS with

10 CPSs. For the summer–autumn cycle, sampling was conducted at 53 DAS with 10 CPSs; the second at 77 DAS with 10 CPSs; the third at 92 DAS with 10 CPSs.

2.4. Laboratory Analysis of Samples

All CPSs were dried in an oven at 65 °C until they all reached a constant weight. Each CPS was then ground using a 0.5 mm mesh. The Dumas method was used to determine the percentage of Nt in each sample. According to Sweeney and Rexroad [34], the determination of Nt is made by thermal conductivity. This method transforms all N into N gas by calcination; the gases produced are reduced by copper, and subsequently desiccated, while the CO_2 (Carbon Dioxide) is trapped. The N is quantified using a Universal Quantifier. The plant samples were processed in the soil laboratory of the Centro Nacional de Investigación Disciplinaria—Relación Agua Suelo Planta Atmósfera (CENID-RASPA), located in Gomez Palacio, Durango. The sampling process was adjusted to the protocol proposed by the Compendium of International Methods of Analysis [35].

2.5. Aerial Imaging

The UAV missions were carried out after maize plants had four fully expanded leaves; this phenotypic stage represents the exponential start of the vegetative development curve. Twelve UAV missions were flown in each of the three production cycles. The UAV was equipped with a Parrot sequoia camera that has the capacity to record up to four wavelength ranges: from 530 to 570 nm (green); 640 to 680 nm (red); 730 to 740 nm (red edge); 770 to 810 nm (near-infrared). The spatial resolution of the multispectral image is 1.2 megapixels. The camera also includes a red, blue, and green (RGB) sensor, with a resolution of 16 megapixels. Regardless of the lighting conditions, the camera has a luminosity sensor in its upper section that allows it to obtain accurate images [36]. The UAV's height above the ground was 191 m; this, along with the camera's field of view, yielded images that represented a ground spatial distance of 18 cm. The images from the UAV missions were captured in EMOTION software (an image processing and flight management platform). Orthomosaic and reflectance values were obtained with Pix4Dmapper software 4.5. The spectral indices obtained from the UAV missions are shown in Table 1.

Table 1. Spectral indices are derived from aerial images.

Index	Equation	Reference
NDRE: sensitive to chlorophyll content when crops are in medium to late stages.	$\left(\frac{NIR-RE}{NIR+RE}\right)$	[37]
CCCI: based on a two-dimensional approach relating the NDVI [38] used to estimate canopy cover, and the NDRE.	$\left(\frac{NDRE}{NDVI}\right)$	[37]
CCCI_simpl: estimates chlorophyll content with minimal sensitivity to other factors that can influence in the canopy signal of N.	$\frac{NDRE-NDRE\ MIN}{NDRE\ MAX-NDRE\ MIN}$	[39]
CI_rededge: indicates chlorophyll content; value shows low sensitivity to the background effects of the soil.	$\left(\frac{NIR}{RE}\right)-1$	[40]
MCARI/OSAVI: very sensitive to variations in chlorophyll content and highly resistant to variations in Leaf Area Index (LAI); takes into account the effects of the soil.	$\frac{\{[(RE-R)-0.2(RE-G)]\left(\frac{RE}{R}\right)\}}{\left[\frac{(1+0.16)(NIR-R)}{NIR+R+0.16}\right]}$	[41]

Table 1. *Cont.*

Index	Equation	Reference
MCARI/OSAVI RE: very sensitive to variations in chlorophyll content and highly resistant to variations in LAI; takes into account the effects of the soil and RE.	$\frac{\left\{[(NIR-RE)-0.2(NIR-G)]\left(\frac{NIR}{RE}\right)\right\}}{\left[\frac{(1+0.16)(NIR-RE)}{NIR+RE+0.16}\right]}$	[42]
TCARI/OSAVI: reduces the effect of soil contribution and enhances sensitivity to chlorophyll content	$3\left\{\frac{\left[(RE-R)-0.2(RE-G)\left(\frac{RE}{R}\right)\right]}{\left[\frac{(1+0.16)(NIR-R)}{NIR+R+0.16}\right]}\right\}$	[43]
TCARI/OSAVI RE: very sensitive to variations in chlorophyll content and highly resistant to variations in LAI; takes into account the effects of the soil and RE.	$3\left\{\frac{\left[(NIR-RE)-0.2(NIR-G)\left(\frac{NIR}{RE}\right)\right]}{\left[\frac{(1+0.16)(NIR-RE)}{NIR+RE+0.16}\right]}\right\}$	[42]
MTCI: has the advantage of being sensitive to N with relatively lesser effect of water or irrigation level for corn.	$\frac{NIR-RE}{RE-R}$	[44]
GNDVI: estimates photosynthetic activity and is a commonly used vegetation index to determine water and N uptake into the plant canopy.	$\frac{NIR-G}{NIR+G}$	[45]
CI_green: estimates chlorophyll content in leaves using the ratio of reflectivity in the NIR and green bands.	$\frac{NIR}{G}-1$	[46]
NDVI: determines the green biomass during the early and middle development stages.	$\frac{NIR-R}{NIR+R}$	[38]
RVI: estimates and monitors green biomass, specifically, in the coverage of high vegetation density.	NIR/R	[47]

NIR: Near Infrared; *RE*: Red Edge; *G*: Green; *R*: Red.

2.6. Data Analysis

The RF decision tree classifier was used to ascertain the link between the Nt data obtained in the laboratory and the value of spectral indices derived from the aerial images. RF can develop multidimensional and multicollinear analyses on large databases [48] and is a suitable data mining technique to estimate Nt in crops [49,50]. The RF implementation was in the Python (v 3.8.0) ecosystem. The outputs of this implementation are a set of decision trees. On this, the contribution of each variable to the model is identified hierarchically. The decision tree is a flowchart, where each of the internal nodes represents an attribute, each branch represents the output of the attribute, and each sheet is a class label. The model developed included independent variables (x = vegetation indices) and a dependent variable (y = Nt). The parameters to quantify the precision and analyze the quality of the input data were declared as follows:

n_estimators. Declares the number of trees in the forest. A greater number of trees improves the accuracy of the data (RF learns faster as more decision trees are included) [25]; however, a too-large number of trees can encourage RF's implementation during the training process. In the model run, the computing process limits were set at 30, 50, 100, 500, 1000, 1500, 2000, 2500, 3000, 3500, and 4000 trees. These thresholds have been used to evaluate RF's abilities [12,51].

max depth. Represents the depth of each tree in the forest. If the tree is deeper, it has more divisions and can capture more information from the data. Its value ranges from 1 to 32.

min_samples_split. Some samples are required to separate a node. Its value ranges from 10% to 100% of the samples.
min_samples_leaf. A minimum number of samples required in the node. Its value ranges from 10% to 50%.
max_features. Number of characteristics to consider when looking for the best node division (default is Auto).

The importance parameter was used to reduce the noise effect of uncorrelated variables. This means that the indices that have the highest correlation in the prediction can be selected and resultin a reduction in computing time. To reduce the number of indices, the model was first trained using all vegetation indices as input variables. Subsequently, based on the importance parameter, all with the lowest weight were eliminated to improve the accuracy of the model and make it more robust.

The optimization of nonparametric regression methods uses a training data-based learning process, which builds a model. The model parameters are adjusted to minimize the estimation error of the extracted variables [52]. A k-fold hold-out cross-validation method with 5 subsets was applied to evaluate the performance of the predictive model. This method has been widely used to validate machine learning models such as RF [12,28,29,52–55] and consists of dividing the entire dataset into two subsets; the first one is to train or adjust the model and while the second one is to validate it [56]. Thus, a model is generated only for training data, which is compared with the data that were reserved for validation and was not used during the development of the model. In the present study, we used 70% of the data for adjustment and 30% for validation. These percentages of data division are similar to those reported by other authors [12,29,53,54,57].

To avoid overfitting and to optimize the performance of the RF, it is necessary to use the n_estimators and max_features hyperparameters. Different combinations of these hyperparameters are carried out in the training stage to obtain the best performance. However, this can cause overfitting, causing the model to perform well on the training set but poorly on the test set. Therefore, it is necessary to perform the cross-validation k-fold [12,28,55]. Firstly, the dataset was divided into training and test sets. In k-fold, only the training set was used and was divided into five subsets. These subsets were iterated using one-fifth of the samples to validate the model and the remaining samples (four-fifths) for training. The first iteration of the first subset was chosen to perform the validation and the four remaining iterations for training. In the second iteration, the second subset was used for validation and subsets one, three, four, and five for training, and so on until the five iterations were computed. The above indicates that five independent pieces of training are carried out to validate the model and that the final accuracy will be the average of the five previous accuracies.

The Nt estimated by the RF model and the Nt calculated in the laboratory were intercompared. The determination coefficient (R^2) and the mean square error was used.

3. Results

3.1. Sampling Universe

The dataset included data from 162 field-collected points and twelve flight missions. The resulting data included Nt (%) obtained from laboratory processing (NLab) of the field samples, and the RF estimated Nt values from five (N_5) and thirteen (N_{13}) spectral indices (Table 2).

Table 2. Results of total Nitrogen content (Nt) (from field sampling) and estimated Nt using Random Forest (RF) (with five and thirteen indices derived from Unmanned Aerial Vehicles (UAVs)) corresponding to Farm and Production cycle, Maize hybrid, and Flight date.

					RF Estimates	
Farm and Production Cycle	**Maize Hybrid**	**Number CPS ***	**Nitrogen$_{Lab}$ (N_{lab}) ****	**Flight Date**	**Nitrogen$_5$ (N_5) †**	**Nitrogen$_{13}$ (N_{13}) ‡**
Granada: Summer–Autumn 2017	Pioneer P3201	15	3.63	11 September 2017	3.56	3.57
		19	2.60	5 October 2017	2.55	2.63
		18	2.53	10 October 2017	2.67	2.63
		16	3.10	20 October 2017	3.04	2.90
		18	2.92	30 October 2017	2.88	2.93
		17	2.46	22 November 2017	2.69	2.53
El Porvenir: Spring–Summer 2018	Syngenta N83N5	10	3.36	28 April 2018	3.39	3.42
		10	2.49	8 May 2018	2.60	2.60
		10	1.75	18 May 2018	1.92	2.02
El Porvenir: Summer–Autumn 2018	Syngenta N83N5	10	1.58	20 September 2018	1.79	1.79
		10	1.23	15 October 2018	1.24	1.23
		10	1.04	30 October 2018	1.22	1.27

* Number CPS refers to the total composite plant samples taken on the farms. ** Nitrogen$_{Lab}$ is the average of the calculated values of Nt in the laboratory. † N_5 is the estimated value of Nt of the five vegetation indices with the greatest contribution to the importance value. ‡ N_{13} is the estimated value of Nt using the thirteen proposed indices.

3.2. Estimate of Nt in Laboratory

The Nt ranged from 0.81% to 4.09% with an average of 2.51% for the 2 years of the study. In the summer–autumn 2017 cycle (n = 103, mean = 2.85%, median = 2.74%, minimum value = 1.8%, maximum value = 4.04%), spring–summer 2018 cycle (n = 30, mean = 2.53%, median = 2.35%, minimum value = 1.53%, maximum value = 4.09%), and summer–autumn 2018 cycle (n = 29, mean = 1.29, median = 1.24%, minimum value = 0.81%, maximum value = 1.96%; Figure 2).

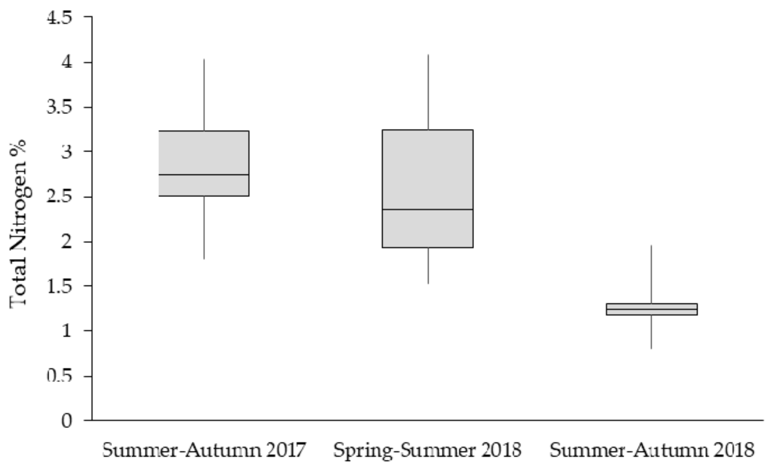

Figure 2. Percent Nt values of field samples measured in the laboratory. The minimum, maximum (vertical bars), and median (solid lines) are displayed.

The Nt values for summer–autumn 2018 were lower than those for summer–autumn 2017, possibly due to the use of two different hybrids and two different study sites. The summer–autumn period at Granada and the Pioneer P3201 hybrid was used because, in the past, they have resulted in a greater range of nitrogen concentration.

3.3. RF Model Optimization

As shown in Figure 3, r^2 raised and dropped dramatically when the model was tried in 100 trees, and subsequently raised again to 1000 and remained almost sustained. When tried in 3000 trees it raised slightly, but if this value is chosen to optimize the n_estimators parameter it can cause an overfitting and slow down the model. In order to avoid the overfitting, 1000 trees were used as an entrance parameter.

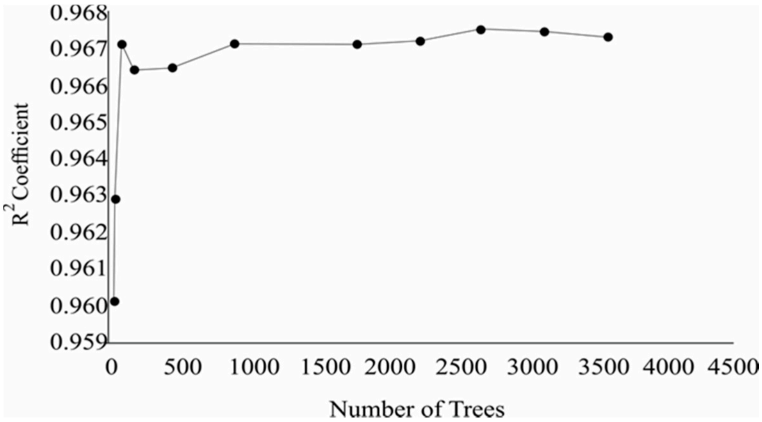

Figure 3. Number of trees according to the R^2 coefficient obtained from RF. The graph corresponds to the area under the curve.

3.4. Validation

Cross-validation results: k-fold with five subsets was $r^2 = 0.76$, while individual accuracies resulted in (−0.52977942, −0.08294489, −1.34383388, −1.77652506, −10.38701745) and a final accuracy of [−2.82 (+/− 7.66)], the first value from the final accuracies shows the average from the individual accuracies, meanwhile the second value represents the standard deviation. Because the data of this study were taken in different crop phenological phases, it can be assumed that is the reason why values are different between stages.

3.5. Selection of the Spectral Indices Based on the Parameter of Importance

Two RF iterations were implemented. In the first, all thirteen indices were included, while in the second all those with the best contribution to the value of importance were selected (Figure 4). In the second iteration, one redundancy effect from minor importance indices was assumed. The TCARI/OSAVI, CI_green, TCARI/OSAVI RE, GNDVI, and NDVI indices were included, which together make up 0.8 of the importance value. Given the decrease in the number of indices, these five improved the value of importance; however, they were not as relevant (0.60, 0.06, 0.05, 0.05, and 0.04, respectively). In this second performance, the TCARI/OSAVI registered the highest importance values in the two runs (0.66).

The scatter plot (Figure 5) shows the relationship between Nt measured in the laboratory and that estimated using thirteen spectral indices, reaching an R^2 of 0.74 with a mean square error (MSE; indicator of model accuracy) of 0.18 (Figure 5a). On the Figure 5b shows that when using the five most important spectral indices, R^2 increased to 0.77 and MSE decreased to 0.15.

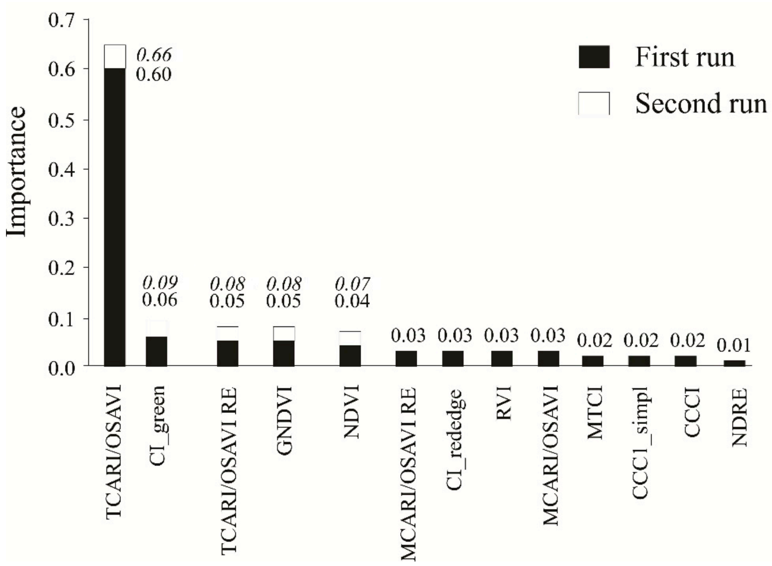

Figure 4. Implementation of two iterations of RF to explore the individual contribution of the explanatory variables according to their importance value to the estimation of Nt. The numbers in italics correspond to the importance value of the five most important variable in the second iteration.

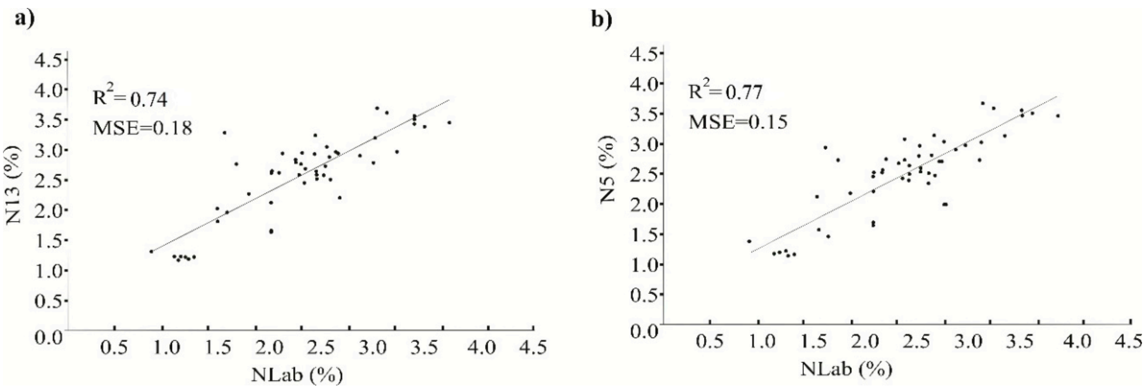

Figure 5. RF prediction for Nt; (**a**) prediction using thirteen indices in the model; (**b**) prediction using five indices in the model.

4. Discussion

During the growing season, any vegetation indices are useful to characterize the phenotypic stages. It has been stated recently that the spectral indices are of fundamental use as a dataset in digital and precision agriculture systems. In determining the Nt [58], the technologies applied to quantify N must be accurate and robust [59,60]. At the production scale, obtaining a more accurate estimation of Nt involves combining methods and processes, in addition to analyzing large datasets—data mining techniques are an example. These technologies are expected to revolutionize agriculture, enabling decision-making in hours or days instead of weeks or months, envisioning a significant reduction in cost and an increase in crop yield [61].

It is broadly recognized and documented that remote sensing has been widely applied in weed mapping, crop growth monitoring, including the health indices of open ecosystems, irrigation management, and many other applications associated with good production practices in most of the production systems. Their use in precision farming practices is diverse and on the rise. The thematic indices show the plant water and/or nutritional needs, plant stress (biotic and nonbiotic), dynamism in time and scale of the geographic space as it occurs, and in general terms, the exchange process among soil cover and the atmosphere. In this manuscript, the indices obtained from high spatial resolution images were useful to estimate the Nt total in forage maize, a crop which is highly sensitive to the N content, but also highly sensitive to the many sources that cause biotic and the abiotic stress, especially during the flowering stage. The RF analysis showed that the TCARI/OSAVI index is the optimal multispectral vegetation index for Nt estimation in forage maize (i.e., R^2 = 0.77). This result is similar to the previous findings of Inoue et al. [62] and Yao et al. [63], who noticed that a combination in indices of NIR and RE bands provides an efficient approach of N status in a plant.

Our results seem to corroborate what was written by Hunt et al. [64] on wheat, that there is a better relationship between the chlorophyll content when the indices utilize the reflectance in the RE wavelengths in comparison to those that do not use it. While some studies about phenotypic characterization and monitoring of corn cultivation have documented the close relationship between the RE band and chlorophyll content [3,5,8,21,22], in this one, the CCCI and NDRE indices showed a weak relationship with Nt; this is contrary to the results documented by authors who report strong relationships with parameters associated with Nt in the plant [65,66]. Nevertheless, this opposite relationship could be associated with conditions of hydric stress, and plant density, as suggested by Rodríguez et al. [67]; though, our results match with those reported by Fitzgerald [68], that the CCCI_simpl index has limited importance in estimating the status of Nt and chlorophyll content in wheat. Comparable results were observed for MCARI/OSAVI and MCARI/OSAVI RE. This study shows the importance of good practices in forage maize to avoid water and nutritional stress.

Results suggest that indices with the RE bandwidth (CCCI_simpl, MCARI/OSAVI, and MCARI/OSAVI RE) are not associated with a stress condition, and also are poorly associated in estimating the Nt in forage maize. Furthermore, more studies are necessary to record additional meteorological variables to vegetation indices, such as the temperature of the air, and the relative humidity to explore their role in conjunction with the vegetation indices with RE bandwidth with maize growth and Nt estimation.

The very positive result is related to the TCARI/OSAVI index. We found a moderate to a strong relationship in estimating the Nt in forage maize. This result matches a study by Chen et al. [22], where they found a relationship between the TCARI/OSAVI and the Nt in corn (R^2 = 0.66), while Berni et al. [10] reported that the TCARI/OSAVI index minimizes the effect of bare soil and variation of leaf area in olive trees, providing predictive relationships to estimate chlorophyll concentration using multispectral imaging. One study unveiled TCARI/OSAVI as very sensitive to estimate the chlorophyll content and is the least sensitive to variations in the Leaf Area Index (LAI) [69]. The robust relationship can be explained by the inclusion of the RE region where chlorophyll exhibits the lowest absorption rate. Therefore, the use of this band in indices reduces the saturation effect on the index, and the reflectance remains sensitive to moderate to high chlorophyll values [3,8,20]. The component that divides the TCARI index from the OSAVI index is the one that considers the contribution of bare soil to the reflectance value. The combination of both indices improves the estimation of Nt in forage maize.

Due to the evident contrast in the importance value of TCARI/OSAVI concerning the thirteen evaluated indices, a specific pattern is visualized in estimating Nt in forage maize much better than the resulting from indices associated with the crop topology such as GNDVI, NDVI, and RVI. These results seem also to support that these structural indices have a weak prediction power to estimate Nt in essence because of the tendency to exhibit saturation values in moderate to high ground cover conditions [5,70,71].

5. Conclusions

Monitoring the growing season of forage maize through field data collection and UAV-based images was a technical challenge because of the high demand for storage and computing resources. In this manuscript, we explored the usefulness of RF analysis to demonstrate whether or not Nt in forage maize plants could be estimated using remotely sensed data. Multispectral image indices were selected to reflect the plant phenology and Nt. The data analysis showed the notable association between the TCARI/OSAVI index (obtained from the RE wavelength) and the Nt in forage maize. We observed that this index enhanced the performance even in comparison with other indices with RE bandwidth included. The five-variable model prediction reached a value of $R^2 = 0.77$ with an MSE of 0.15. This study opens new avenues to support precision farming decision making in irrigated-water crops.

Author Contributions: Conceptualization, M.J.L.-C., J.E.-Á. and V.M.R.-M.; Data curation, M.J.L.-C., J.E.-Á. and J.E.M.-R.; Formal analysis, V.M.R.-M.; Investigation, M.J.L.-C., G.D.-R. and E.M.-V.; Methodology, M.J.L.-C., J.E.-Á., V.M.R.-M. and J.E.M.-R.; Resources, J.E.-Á. and V.M.R.-M.; Visualization, A.R.M.-S.; Writing—original draft, V.M.R.-M. and A.R.M.-S.; Writing—review and editing, J.E.-Á. and V.M.R.-M. All authors have read and agreed to the published version of the manuscript.

Funding: This research was funded by Proyecto piloto de apoyo a la agricultura para el uso de la radiación solar en la producción alimentaria, grant number No: 16474434651 and Incremento en el uso eficiente del agua, a través de tecnologías digitales de fácil acceso y adopción en las zonas agrícolas de Zacatecas y la Comarca Lagunera, grant number No: 10221634653.

Conflicts of Interest: The authors declare no conflict of interest.

References

1. Sage, R.F.; Pearcy, R.W. The Nitrogen Use Efficiency of C3 and C4 Plants: II. Leaf Nitrogen Effects on the Gas Exchange Characteristics of *Chenopodium album* (L.) and *Amaranthus retroflexus* (L.). *Plant Physiol.* **1987**, *84*, 959–963. [CrossRef] [PubMed]
2. Vos, J.; Putten, P.E.L.; Birch, C.J. Effect of nitrogen supply on leaf appearance, leaf growth, leaf nitrogen economy and photosynthetic capacity in maize (*Zea mays* L.). *Field Crop. Res.* **2005**, *93*, 64–73. [CrossRef]
3. Clevers, J.G.P.W.; Gitelson, A.A. Remote estimation of crop and grass chlorophyll and nitrogen content using red-edge bands on Sentinel-2 and -3. *Int. J. Appl. Earth Obs. Geoinf.* **2013**, *23*, 344–351. [CrossRef]
4. Sánchez, A.; Delgado, R.; Lorbes, J.; Rodríguez, V.; Figueredo, L.; Gómez, C. Diagnóstico e índice para fertilización nitrogenada en etapa vegetativa del cultivo maíz (*Zea mays* L.). *Revista Unellez de Ciencia y Tecnología* **2015**, *33*, 75–82.
5. Basso, B.; Fiorentino, C.; Cammarano, D.; Schulthess, U. Variable rate nitrogen fertilizer response in wheat using remote sensing. *Precis. Agric.* **2015**, *17*, 168–182. [CrossRef]
6. Li, F.; Miao, Y.; Feng, G.; Yuan, F.; Yue, S.; Gao, X.; Liu, Y.; Liu, B.; Ustin, S.L.; Chen, X. Improving estimation of summer maize nitrogen status with red edge-based spectral vegetation indices. *Field Crop. Res.* **2014**, *157*, 111–123. [CrossRef]
7. Cruz Durán, J.A.; Sánchez García, P.; Galvis Spínola, A.; Carrillo Salazar, J.A. Índices espectrales en pimiento para el diagnóstico nutrimental de nitrógeno. *Terra Latinoam.* **2011**, *29*, 259–265.
8. Schlemmer, M.; Gitelson, A.; Schepers, J.; Ferguson, R.; Peng, Y.; Shanahan, J.; Rundquist, D. Remote estimation of nitrogen and chlorophyll contents in maize at leaf and canopy levels. *Int. J. Appl. Earth Obs. Geoinf.* **2013**, *25*, 47–54. [CrossRef]
9. Simic Milas, A.; Romanko, M.; Reil, P.; Abeysinghe, T.; Marambe, A. The importance of leaf area index in mapping chlorophyll content of corn under different agricultural treatments using UAV images. *Int. J. Remote Sens.* **2018**, *39*, 5415–5431. [CrossRef]
10. Berni, J.; Zarco-Tejada, P.J.; Suarez, L.; Fereres, E. Thermal and Narrowband Multispectral Remote Sensing for Vegetation Monitoring from an Unmanned Aerial Vehicle. *IEEE Trans. Geosci. Remote Sens.* **2009**, *47*, 722–738. [CrossRef]
11. Tan, C.; Du, Y.; Zhou, J.; Wang, D.; Luo, M.; Zhang, Y.; Guo, W. Analysis of Different Hyperspectral Variables for Diagnosing Leaf Nitrogen Accumulation in Wheat. *Front. Plant Sci.* **2018**, *9*, 674. [CrossRef] [PubMed]
12. Abdel-Rahman, E.M.; Ahmed, F.B.; Ismail, R. Random forest regression and spectral band selection for estimating sugarcane leaf nitrogen concentration using EO-1 Hyperion hyperspectral data. *Int. J. Remote Sens.* **2013**, *34*, 712–728. [CrossRef]
13. Zheng, H.; Li, W.; Jiang, J.; Liu, Y.; Cheng, T.; Tian, Y.; Zhu, Y.; Cao, W.; Zhang, Y.; Yao, X. A Comparative Assessment of Different Modeling Algorithms for Estimating Leaf Nitrogen Content in Winter Wheat Using Multispectral Images from an Unmanned Aerial Vehicle. *Remote Sens.* **2018**, *10*, 2026. [CrossRef]
14. Lukas, V.; Novák, J.; Neudert, L.; Svobodova, I.; Rodriguez-Moreno, F.; Edrees, M.; Kren, J. The Combination of Uav Survey and Landsat Imagery for Monitoring of Crop Vigor in Precision Agriculture. *ISPRS Int. Arch. Photogramm. Remote Sens. Spat. Inf. Sci.* **2016**, *XLI-B8*, 953–957. [CrossRef]

15. Barber, J.; Horler, D.N.H. *Fundamental Relationships between Plant Spectra and Geobotanical Stress Phenomena*; NAS5-23738; NASA, Goddard Space Flight Center: Greenbelt, MD, USA, 1981. Available online: https://ntrs.nasa.gov/archive/nasa/casi.ntrs.nasa.gov/19810015964.pdf#page=43 (accessed on 5 January 2020).
16. Ferns, D.C.; Zara, S.J.; Barber, J. Application of high resolution spectroradiometry to vegetation. *Photogramm. Eng. Remote Sens.* **1984**, *50*, 1725–1735.
17. Salisbury, J.W.; Milton, N.M.; Walsh, P.A. Significance of non-isotropic scattering from vegetation for geobotanical remote sensing. *Int. J. Remote Sens.* **1987**, *8*, 997–1009. [CrossRef]
18. Horler, D.N.H.; Dockray, M.; Barber, J. The red edge of plant leaf reflectance. *Int. J. Remote Sens.* **1983**, *4*, 273–288. [CrossRef]
19. Curran, P.J.; Dungan, J.L.; Gholz, H.L. Exploring the relationship between reflectance red edge and chlorophyll content in slash pine. *Tree Physiol.* **1990**, 33–48. [CrossRef]
20. Raper, T.B.; Varco, J.J. Canopy-scale wavelength and vegetative index sensitivities to cotton growth parameters and nitrogen status. *Precis. Agric.* **2014**, *16*, 62–76. [CrossRef]
21. Schlemmer, M.R.; Francis, D.D.; Shanahan, J.F.; Schepers, J.S. Remotely Measuring Chlorophyll Content in Corn Leaves with Differing Nitrogen Levels and Relative Water Content. *Agron. J.* **2005**, *97*, 106–112. [CrossRef]
22. Chen, P.; Haboudane, D.; Tremblay, N.; Wang, J.; Vigneault, P.; Li, B. New spectral indicator assessing the efficiency of crop nitrogen treatment in corn and wheat. *Remote Sens. Environ.* **2010**, *114*, 1987–1997. [CrossRef]
23. Feng, W.; Wu, Y.; He, L.; Ren, X.; Wang, Y.; Hou, G.; Wang, Y.; Liu, W.; Guo, T. An optimized non-linear vegetation index for estimating leaf area index in winter wheat. *Precis. Agric.* **2019**. [CrossRef]
24. Prabhakara, K.; Hively, W.D.; McCarty, G.W. Evaluating the relationship between biomass, percent groundcover and remote sensing indices across six winter cover crop fields in Maryland, United States. *Int. J. Appl. Earth Obs. Geoinf.* **2015**, *39*, 88–102. [CrossRef]
25. Fraj, M.B. In Depth: Parameter Tuning for Random Forest 2019. Available online: https://medium.com/all-things-ai/in-depth-parameter-tuning-for-random-forest-d67bb7e920d (accessed on 21 December 2019).
26. Krishna, G.; Sahoo, R.N.; Singh, P.; Bajpai, V.; Patra, H.; Kumar, S.; Dandapani, R.; Gupta, V.; Viswanathan, C.; Ahmad, T.; et al. Comparison of various modelling approaches for water deficit stress monitoring in rice crop through hyperspectral remote sensing. *Agric. Water Manag.* **2019**, *213*, 231–244. [CrossRef]
27. Pham, T.; Yokoya, N.; Tien, D.; Yoshino, K.; Friess, D. Remote Sensing Approaches for Monitoring Mangrove Species, Structure, and Biomass: Opportunities and Challenges. *Remote Sens.* **2019**, *11*, 230. [CrossRef]
28. Shah, S.; Angel, Y.; Houborg, R.; Ali, S.; McCabe, M. A Random Forest Machine Learning Approach for the Retrieval of Leaf Chlorophyll Content in Wheat. *Remote Sens.* **2019**, *11*, 920. [CrossRef]
29. Mutanga, O.; Adam, E.; Cho, M.A. High density biomass estimation for wetland vegetation using WorldView-2 imagery and random forest regression algorithm. *Int. J. Appl. Earth Obs. Geoinf.* **2012**, *18*, 399–406. [CrossRef]
30. Hastie, T.; Friedman, J.; Tibshirani, R. *The Elements of Statistical Learning*; Springer Series in Statistics; Springer: New York, NY, USA, 2001. [CrossRef]
31. Rodriguez-Galiano, V.F.; Ghimire, B.; Rogan, J.; Chica-Olmo, M.; Rigol-Sanchez, J.P. An assessment of the effectiveness of a random forest classifier for land-cover classification. *ISPRS J. Photogramm. Remote Sens.* **2012**, *67*, 93–104. [CrossRef]
32. Galindo, G.A.; Cabrera, E.; Vargas, D.M.; Pabón, H.R.; Cabrera, K.R.; Yepes, A.P.; Phillips, J.F.; Navarrete, D.A.; Duque, A.J.; García, M.C.; et al. *Estimación de la Biomasa Aérea Usando Datos de Campo e Información De Sensores Remotos*; Instituto de Hidrología, Meteorología, y Estudios Ambientales (IDEAM): Bogotá, Colombia, 2011; 52p. Available online: http://www.ideam.gov.co/documents/13257/13548/Biomasa+Sensores.pdf/1ad2a058-1b6f-48c1-b826-f2625eed610e (accessed on 5 January 2020).
33. SIAP.SAGARPA. Servicio de Información Agroalimentaria y Pesquera 2018. Available online: http://www.siap.gob.mx/ (accessed on 20 December 2019).
34. Sweeney, R.A.; Rexroad, P.R. Comparison of LECO FP-228 'Nitrogen Determinator' with AOAC copper catalyst Kjeldahl method for crude protein. *J. AOAC* **1987**, *70*, 1028–1030.
35. OIV-(International Organisation of Vine and Wine). *Quantification of Total Nitrogen According to the Dumas Method (Musts and Wines)*; Compendium of International Methods of Wine and Must Analysis; OIV: Paris, France, 2012; Volume 2, Available online: http://www.oiv.int/public/medias/2578/oiv-ma-as323-02a.pdf (accessed on 15 December 2019).

36. Parrot. Paris, France. Available online: https://www.parrot.com/business-solutions-us/parrot-professional/parrot-sequoia (accessed on 26 November 2019).
37. Barnes, E.M.; Clarke, T.R.; Richards, S.E.; Colaizzi, P.D.; Haberland, J.; Kostrewski, M.; Waller, P.; CHoi, C.; Riley, E.; Tompson, T.; et al. Coincident detection of crop water stress, nitrogen status and canopy density using ground-based multispectral data. In Proceedings of the 5th International Conference on Precision Agriculture, Bloomington, MN, USA, 16–19 July 2000; ASA-CSSA-SSSA: Madison, WI, USA, 2000. Available online: http://citeseerx.ist.psu.edu/viewdoc/download?doi=10.1.1.463.8007&rep=rep1&type=pdf (accessed on 10 June 2017).
38. Rouse, J.W.; Has, R.H.; Schell, J.A.; Deering, D.W. Monitoring vegetation systems in the great plains with ERTS. In *Third ERTS Symposium, NASA SP-351, Vol. 1*; NASA: Washington, DC, USA, 1974; pp. 309–317. Available online: https://ntrs.nasa.gov/archive/nasa/casi.ntrs.nasa.gov/19740022614.pdf (accessed on 11 June 2017).
39. Fitzgerald, G.; Rodriguez, D.; O'Leary, G. Measuring and predicting canopy nitrogen nutrition in wheat using a spectral index—The canopy chlorophyll content index (CCCI). *Field Crop. Res.* **2010**, *116*, 318–324. [CrossRef]
40. Gitelson, A.A.; Gritz, Y.; Merzlyak, M.N. Relationships between leaf chlorophyll content and spectral reflectance and algorithms for non-destructive chlorophyll assessment in higher plant leaves. *J. Plant Physiol.* **2003**, *160*, 271–282. [CrossRef] [PubMed]
41. Daughtry, C. Estimating Corn Leaf Chlorophyll Concentration from Leaf and Canopy Reflectance. *Remote Sens. Environ.* **2000**, *74*, 229–239. [CrossRef]
42. Wu, C.; Niu, Z.; Tang, Q.; Huang, W. Estimating chlorophyll content from hyperspectral vegetation indices: Modeling and validation. *Agric. For. Meteorol.* **2008**, *148*, 1230–1241. [CrossRef]
43. Haboudane, D.; Miller, J.R.; Tremblay, N.; Zarco-Tejada, P.J.; Dextraze, L. Integrated narrow-band vegetation indices for prediction of crop chlorophyll content for application to precision agriculture. *Remote Sens. Environ.* **2002**, *81*, 416–426. [CrossRef]
44. Dash, J.; Curran, P.J. The MERIS terrestrial chlorophyll index. *Int. J. Remote Sens.* **2010**, *25*, 5403–5413. [CrossRef]
45. Gitelson, A.A.; Merzlyak, M.N. Signature Analysis of Leaf Reflectance Spectra: Algorithm Development for Remote Sensing of Chlorophyll. *J. Plant Physiol.* **1996**, *148*, 494–500. [CrossRef]
46. Gitelson, A.A. Remote estimation of canopy chlorophyll content in crops. *Geophys. Res. Lett.* **2005**, *32*. [CrossRef]
47. Jordan, C.F. Derivation of Leaf-Area Index from Quality of Light on the Forest Floor. *Ecology* **1969**, *50*, 663–666. [CrossRef]
48. Belgiu, M.; Drăguţ, L. Random forest in remote sensing: A review of applications and future directions. *ISPRS J. Photogramm. Remote Sens.* **2016**, *114*, 24–31. [CrossRef]
49. Li, X.Q.; Liu, X.N.; Liu, M.L.; Wu, L. Random forest algorithm and regional applications of spectral inversion model for estimating canopy nitrogen concentration in rice. *J. Remote Sens.* **2014**, *18*, 923–945. [CrossRef]
50. Liang, L.; Di, L.; Huang, T.; Wang, J.; Lin, L.; Wang, L.; Yang, M. Estimation of Leaf Nitrogen Content in Wheat Using New Hyperspectral Indices and a Random Forest Regression Algorithm. *Remote Sens.* **2018**, *10*, 1940. [CrossRef]
51. Prasad, A.M.; Iverson, L.R.; Liaw, A. Newer Classification and Regression Tree Techniques: Bagging and Random Forests for Ecological Prediction. *Ecosystems* **2006**, *9*, 181–199. [CrossRef]
52. Liu, Y.; Cheng, T.; Zhu, Y.; Tian, Y.; Cao, W.; Yao, X.; Wang, N. Comparative analysis of vegetation indices, non-parametric and physical retrieval methods for monitoring nitrogen in wheat using UAV-based multispectral imagery. *IEEE Int. Geosci. Remote Sens. Symp.* **2016**. [CrossRef]
53. Han, L.; Yang, G.; Dai, H.; Xu, B.; Yang, H.; Feng, H.; Li, Z.; Yang, X. Modeling maize above-ground biomass based on machine learning approaches using UAV remote-sensing data. *Plant Methods* **2019**, *15*. [CrossRef]
54. Medina-Merino, R.; Ñique-Chacón, C. Bosques aleatorios como extensión de los árboles de clasificación con los programas R y Python. *Interfases* **2017**, 165–189. [CrossRef]
55. Prado Osco, L.; Marquez, A.P.; Roberto, D.; Akemi, É.; Nobuhiro, N.; Takashi, E.; Estrabis, N.; de Souza, M.; Junior, J.M.; Gonçalves, W.N.; et al. Predicting Canopy Nitrogen Content in Citrus-Trees Using Random Forest Algorithm Associated to Spectral Vegetation Indices from UAV-Imagery. *Remote Sens.* **2019**, *11*, 2925. [CrossRef]

56. Arlot, S.; Celisse, A. A Survey of Cross-validation Procedures for Model Selection. *Stat. Surv.* **2010**, *4*, 40–79. [CrossRef]
57. Pérez-Planells, L.; Delegido, J.; Rivera, J.; Verrelst, J. Analysis of cross-validation methods for robust retrieval of biophysical parameters. *Rev. Teledetección* **2015**, *44*, 55–65. [CrossRef]
58. Ye, H.; Huang, W.; Huang, S.; Wu, B.; Dong, Y.; Cui, B. Remote estimation of nitrogen vertical distribution by consideration of maize geometry characteristics. *Remote Sens.* **2018**, *10*, 1995. [CrossRef]
59. Ju, X.; Christie, P. Calculation of theoretical nitrogen rate for simple nitrogen recommendations in intensive cropping systems: A case study on the North China Plain. *Field Crop. Res.* **2011**, *124*, 450–458. [CrossRef]
60. Frels, K.; Guttieri, M.; Joyce, B.; Leavitt, B.; Baenziger, P.S. Evaluating canopy spectral reflectance vegetation indices to estimate nitrogen use traits in hard winter wheat. *Field Crop. Res.* **2018**, *217*, 82–92. [CrossRef]
61. Tsouros, D.C.; Bibi, S.; Sarigiannidis, P.G. A Review on UAV-Based Applications for Precision Agriculture. *Information* **2019**, *10*, 349. [CrossRef]
62. Inoue, Y.; Sakaiya, E.; Zhu, Y.; Takahashi, W. Diagnostic mapping of canopy nitrogen content in rice based on hyperspectral measurements. *Remote Sens. Environ.* **2012**, *126*, 210–221. [CrossRef]
63. Yao, X.; Zhu, Y.; Tian, Y.; Feng, W.; Cao, W. Exploring hyperspectral bands and estimation indices for leaf nitrogen accumulation in wheat. *Int. J. Appl. Earth Obs. Geoinf.* **2010**, *12*, 89–100. [CrossRef]
64. Hunt, E.R.; Daughtry, C.S.T.; Eitel, J.U.H.; Long, D.S. Remote Sensing Leaf Chlorophyll Content Using a Visible Band Index. *Agron. J.* **2011**, *103*, 1090–1099. [CrossRef]
65. Cammarano, D.; Fitzgerald, G.; Basso, B.; O'Leary, G.; Chen, D.; Grace, P.; Fiorentino, C. Use of the Canopy Chlorophyl Content Index (CCCI) for Remote Estimation of Wheat Nitrogen Content in Rainfed Environments. *Agron. J.* **2011**, *103*, 1597–1603. [CrossRef]
66. Eitel, J.U.; Keefe, R.F.; Long, D.S.; Davis, A.S.; Vierling, L.A. Active ground optical remote sensing for improved monitoring of seedling stress in nurseries. *Sensors* **2010**, *10*, 2843–2850. [CrossRef]
67. Rodriguez, D.; Fitzgerald, G.J.; Belford, R.; Christensen, L.K. Detection of nitrogen deficiency in wheat from spectral reflectance indices and basic crop eco-physiological concepts. *Aust. J. Agric. Res.* **2006**, *57*. [CrossRef]
68. Fitzgerald, G.J.; Rodriguez, D.; Christensen, L.K.; Belford, R.; Sadras, V.O.; Clarke, T.R. Spectral and thermal sensing for nitrogen and water status in rainfed and irrigated wheat environments. *Precis. Agric.* **2006**, *7*, 233–248. [CrossRef]
69. Eitel, J.U.H.; Long, D.S.; Gessler, P.E.; Smith, A.M.S. Using in-situ measurements to evaluate the new RapidEye™ satellite series for prediction of wheat nitrogen status. *Int. J. Remote Sens.* **2007**, *28*, 4183–4190. [CrossRef]
70. Duan, T.; Chapman, S.C.; Guo, Y.; Zheng, B. Dynamic monitoring of NDVI in wheat agronomy and breeding trials using an unmanned aerial vehicle. *Field Crop. Res.* **2017**, *210*, 71–80. [CrossRef]
71. Karki, T. Yield prediction and nitrogen recommendation in maize using normalized difference vegetation index. *Agron. J. Nepal* **2013**, *3*, 82–88. [CrossRef]